

Study of defects and impurities in multicrystalline silicon grown from metallurgical silicon feedstock

S. Binetti^{a,*}, J. Libal^a, M. Acciarri^a, M. Di Sabatino^b, H. Nordmark^c, E.J. Øvrelid^b, J.C. Walmsley^{b,c}, R. Holmestad^c

^a University of Milano Bicocca, Department of Materials Science, via Cozzi 53, 20125 Milano, Italy

^b SINTEF Materials and Chemistry, A. Getz v. 2B, 7465 Trondheim, Norway

^c Department of Physics, NTNU, NO-7491 Trondheim, Norway

ARTICLE INFO

Article history:

Received 29 April 2008

Received in revised form 10 May 2008

Accepted 13 May 2008

Keywords:

Metallurgical silicon

Impurities

Gettering

Lifetime

EBIC

Photoluminescence

ABSTRACT

Nowadays the photovoltaic (PV) market suffers the severe shortage of silicon. One possible solution is to produce SoG-Si via a direct metallurgical route, followed by a final casting step. The use of such lower quality materials in solar cell production depends on the possibility of improving the electrical quality during the cell processing and requires a deep understanding of the interaction between defects. The aim of this work is to study the electrical properties and the minority charge carrier recombination behaviour of extended defects in a mc-Si ingot grown from metallurgical Si produced directly by carbothermic reduction of very pure quartz and carbon. The combined application of photoluminescence, infrared spectroscopy, electron beam induced current technique and transmission electron microscopy succeeded in identifying oxygen precipitates, decorated grain boundaries and dislocations as the defects which limit the quality of the metallurgical mc-Si and, therefore, the efficiency of the related solar cells.

© 2008 Elsevier B.V. All rights reserved.

1. Introduction

The increasing interest in renewable energy sources with a low environmental impact has given rise to a rapid growth of the photovoltaic (PV) industry. Up to now, the dominant semiconductor material used in PV is silicon and it is expected that silicon will play a fundamental role at least for the next decade. As the electronics sector recovers, and the requirements of the PV industry expand, there has been an increasing need for a dedicated supply of silicon. On the other hand, the severe shortage of the silicon used in the systems threatens to dampen the PV market's growth. Therefore, a new supply of solar grade silicon (SoG-Si) is crucial. One possible solution is to produce SoG-Si via a direct metallurgical route, followed by a final casting step. The metallurgical grade silicon made by direct reduction of quartz and carbon black is about 98.5% pure [1], i.e. a purity far from the 8 N pure silicon currently used in PV industry. The possibility of using such contaminated material in solar cell production depends on the following factors:

- using extra pure quartz in order to start with a higher quality material;
- improving the electrical quality during the cell processing;
- develop of new device process with less dependence on the quality of the material, i.e., on the diffusion length and on dopant/type.

The possibility of improving the electrical quality before or during the cell process requires a deep understanding of the type and concentration of impurity and defect, the presence of complex and cluster, the effect of impurity segregation process on the electrical activity of extended defects, as the solar cell efficiencies attainable with mc-solar grade Si are determined by all these material properties.

This work deals with a complete characterization of the electrical properties and the minority charge carrier recombination behaviour of extended defects in mc-Si ingots grown from metallurgical Si, produced directly by carbothermic reduction of very pure quartz and carbon without subsequent purification processes. The aim of the work is to test the feasibility of using such material in solar cell standard device process and to show how a combined application of different techniques succeeded in the identification

* Corresponding author. Tel.: +39 0264485177; fax: +39 0264485400.
E-mail address: simona.binetti@unimib.it (S. Binetti).

of the nature of the defects which can limit the efficiency of the final solar cells.

2. Experimental details

The silicon feedstock used has been produced by direct reduction of extra pure quartz and carbon black. After tapping from the reduction furnace, the material was cooled down, etched and cleaned with DI water. The mc-Si ingot was made in a directional solidification lab scale furnace, without any subsequent purification processes. The resulting ingot (diameter 250 mm, height 120 mm, 12 kg) was cut into wafers after a single crystallization step. Details of the furnace and casting experiment were previously given [2]. The lifetime of minority carriers was determined using the quasi-steady-state photoconductance technique (QSSPC) [3]. Before measuring the as-grown samples have been subjected to a polishing etch containing HNO_3 , HF and CH_3COOH and subsequent surface clean by $\text{H}_2\text{O}_2\text{:H}_2\text{SO}_4 = 1\text{:}4$, followed by an HF-Dip. The surfaces of the samples were passivated by an iodine ethanol (IE) solution [4].

The resistivity values were determined at various positions in each wafer and along the ingot height using the 4-point-probe technique [5]. The local recombination activity of extended defects was measured by EBIC at 300 K and down to 100 K. The photoluminescence (PL) spectra were recorded at 14 K with a spectral resolution of 6.6 nm. Details about sample preparation, PL and EBIC techniques are reported in [6]. Finally, the interstitial oxygen [O]_i and substitutional carbon [C]_s concentrations were measured by Fourier transform infrared (FTIR) spectroscopy [7]. The total oxygen concentration was carried out by inert gas fusion method by LECO [8]. In order to test the well-known gettering effect of the phosphorus diffusion step [9,10] on such solar grade silicon, a P-diffusion with POCl_3 in an open-tube furnace was carried out on different wafers. The doped regions were subsequently removed from the samples to carry out lifetime, EBIC and PL measurements. Transmission Electron Microscope (TEM) was used for the high resolution imaging and chemical analysis of precipitates. Experimental details in [11].

3. Results and discussion

Table 1 shows the main properties of the selected wafers from different heights of the ingot (where nr 1 indicates a wafer close to the top while nr 6 close to the bottom of the ingot). The minority carrier-lifetime values in the investigated material are much lower than in standard mc-Si, as one may expect due to a higher concentration of metallic impurities. According to the glow discharge mass spectrometry (GDMS) analysis Al and Fe concentrations were about 1.18 and 0.09 ppmw (at 88 mm from the bottom), respectively and the concentrations of other metallic elements such as Cu, Ni and Ti, were less than 50 ppbw [12,13]. As no doping elements were added during the solidification, and as the doping elements (B, Al, P) present have different segregation coefficient, the resulting ingot was n-type in a small fraction of the top and p-type in the bottom

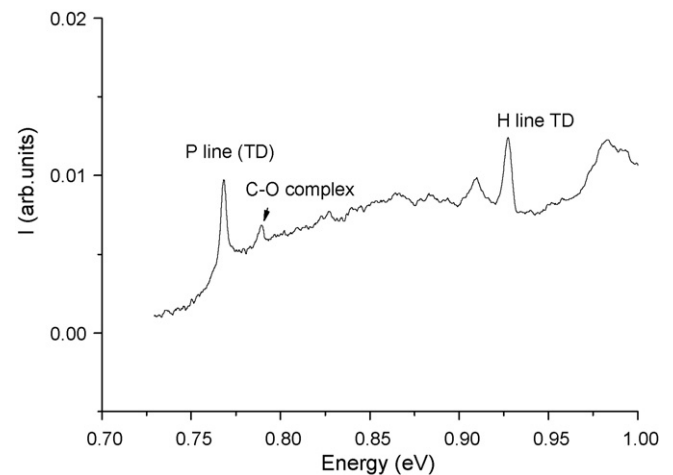


Fig. 1. Typical PL spectrum collected at $T = 12$ K and $P = 6$ W/cm².

part of the ingot. As can be seen from Table 1, the interstitial oxygen concentration is higher than in a standard mc-Si [6,14]. The LECO analysis carried out on the feedstock chunks revealed a total oxygen concentration of about 30 ppmw indicated that one of the major oxygen source is the feedstock itself. This can be explained, by an oxidation process that occurs during the tapping into vessel of the liquid silicon, carried out in air and at high temperature. As the tapping is a discontinuous process, silicon dioxide interface layers can be formed in silicon, becoming an oxygen source during the solidification process.

A typical PL spectrum of the as-grown samples, in the low energy range, is plotted in Fig. 1 and it shows the presence of a peak at approximately 0.77 eV, usually labeled as P line, together with two signals at approximately 0.91 and 0.93 eV, respectively (labeled as H lines) [15,16]. These lines are related to the presence of C–O complex and nuclei of SiO_x , known as old thermal donors (OTD). As the P line luminescence should be related to a transition from a thermal donors (TD) bound excitation level to a deep level corresponding to the C–O complexes [17,18] it could be responsible for a decrease of the minority carrier-lifetime. Evidence was given that thermal donors decrease the minority charge carrier-lifetime in solar grade monocrystalline silicon [14]. While the PL analysis revealed the presence of silicon dioxide nuclei, the presence of silicon dioxide precipitates have been identified by TEM analysis. SiO_2 precipitates were commonly observed in grain boundaries and almost all dislocations were heavily decorated by oxygen precipitates as shown in Fig. 2.

From the EBIC measurements (see Fig. 3), it is evident that, independently by the ingot position, the material is characterised by a high density of active extended defects also at room temperature. In the EBIC maps at 300 K, “bright” denuded zone at GBs are easily visible. This effect is typical of high-contaminated materials and it is due to segregation of metallic impurities at defects [19,20]. Even

Table 1

Sample designations, positions of the wafers in the ingot, resistivity, lifetime, interstitial oxygen and substitutional carbon concentration

Wafer#	Position from bottom (mm)	Resistivity (Ω cm)		Lifetime (μ s)	O _i (ppma)	C _s (ppma)
6-2	16	3.9 (\pm 1.6)	p	1	23.1 (\pm 1.3)	4 (\pm 0.3)
5-2	28	4.6 (\pm 1.6)	p	1	25 (\pm 1.4)	4 (\pm 1.7)
4-2	40	4.2 (\pm 2.5)	p	0.9	27.2 (\pm 2.6)	10 (\pm 0.5)
3-2	52	3.6 (\pm 1.8)	p	1.1	25.6 (\pm 4)	8.8 (\pm 1.6)
2-2	64	4.4 (\pm 3.1)	p	1	24.8 (\pm 3)	7.6 (\pm 2)
1-2	76	4.5 (\pm 4.4)	n	3.2	25 (\pm 3)	12 (\pm 2)

The high standard deviation of average resistivity values measured on different points into a single wafers are related to grain boundaries effect. Lifetime values have been calculated with an excess carriers density between 7×10^{13} and 5×10^{14} cm⁻³. Note that numerical designations are used in the text and figures.

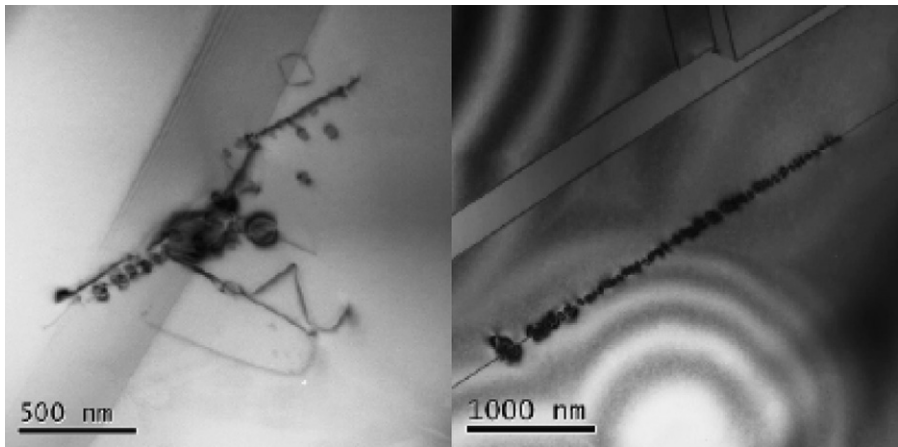


Fig. 2. SiO₂ precipitates located on a dislocation in a grain boundary (left) and SiO₂ platelets edge on in a twin boundary (right).

though the EBIC measurements have no statistical meaning, as the maps are performed on small selected areas of each sample, we saw that the density of bright spots is higher in the top part of the ingots. Furthermore, the average EBIC contrast measured is relatively high (about 30% at RT) and can be also due to the presence of metallic precipitates, confirmed by TEM analysis carried out on the same material [21]. The presence of precipitates is confirmed by the behaviour of contrast versus *T*: at low temperature the GBs contrast

slightly decreases (at about 20%). This effect has been explained on the basis of the Shockley–Read–Hall theory [20] with the presence of a high density of deep levels at the GBs as a consequences of metallic decoration and precipitation.

The effect of the P-diffusion step on the lifetime is reported in Fig. 4. It could be observed that an increase was obtained only for the top part of the ingot. The non-increase of lifetime in other part of the ingot is related to a non-sufficient effectiveness of gettering

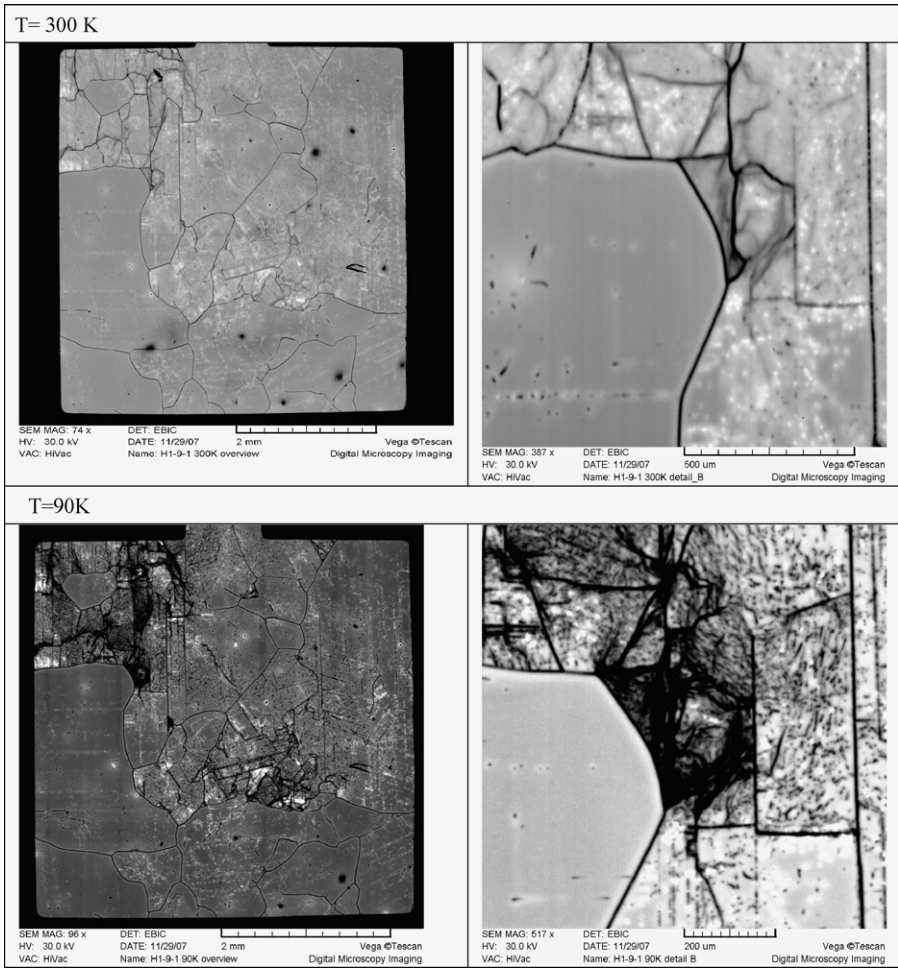


Fig. 3. Low magnification EBIC maps collected at 300 and 90 K for sample #2-2 (left) and high magnification EBIC maps collected at 300 and 90 K for the same sample (right).

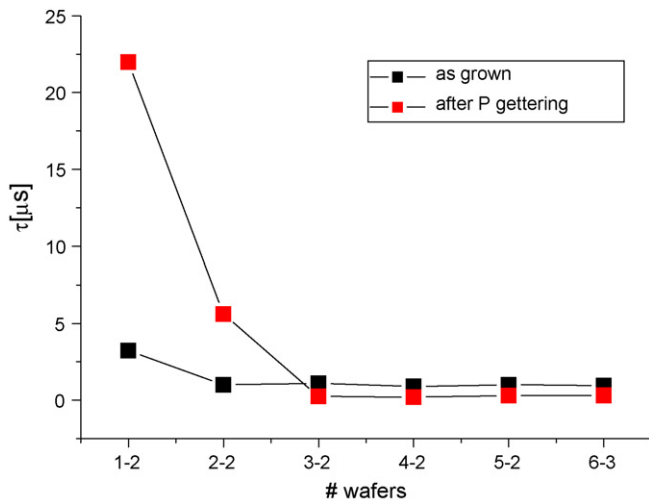


Fig. 4. Change in lifetime along the ingot due to the solar cell processing steps of P-diffusion (sample #1-2 is n-type).

P-diffusion step on these wafers. As the type of metallic impurities is the same along the ingot, this can be only due to a difference in concentration or a difference in extended defects density. The difference in concentration of metallic impurities along the ingot can explain the higher improvement of the top part as already observed in literature but not the constant low lifetime from wafer #3.2 to the bottom part of the ingot. On the one hand, EBSD measurements showed that the grains in the top of the ingot (1-3 to 3-3) are rather large ($\approx 5\text{--}20\text{ mm}$) whereas they are small in the bottom of the ingot (sample 4-3 to 6-3, $<1\text{ mm}$), however, it is not small enough to limit the lifetime to the low values found in these samples after P-gettering. However, EBIC measurements on this material showed that often small grains feature a much higher dislocation density than larger grains do. This problem will be certainly resolved when growing industrial size ingot.

On the other hand, the PL spectra on gettered sample indicate a disappearance of bands associated to nuclei of precipitates, but the interstitial oxygen concentration does not increase indicating the formation of precipitates during the P-diffusion.

According to EBIC, TEM and PL results, it can be inferred that, besides a high dislocation density in the bottom part of the ingot, the main factor responsible of the low quality wafers after the gettering is the presence of high density of oxygen precipitates sometimes decorated with metals. This confirms also that the impurities present in the form of precipitates (oxides and silicides) can not be gettered out by P-diffusion step as already observed in [22].

4. Conclusions

An important aspect pointed out by this work is that the presence of a high oxygen concentration, should be taken into account when using such solar grade silicon for solar cell production. The presence of silicon dioxide precipitates should be avoided. First of all because they show strong recombination activity as verified in monocrystalline silicon [23] but mainly because they

can act as internal gettering sink during the solidification step and device processes. The possibility of using solar grade silicon directly solidified from metallurgical one is not so far and depends mainly on the control of the precipitation process during crystallization (i.e. optimizing the temperature profiles) and on post-solidification annealing able to reduce the density of oxygen or oxygen-containing defect centres. The dissolved metallic impurities are largely gettable by a P-diffusion step and are, therefore, not so harmful for the electrical properties of the material at the end of the solar cell process. PC1D simulations [24] using the carrier-lifetimes measured in wafer #1-2 and # 2-2 after gettering showed that solar cell with efficiency of 12.4 and 13.9%, respectively, could be obtained. Taking into account the high actual cost of Si feedstock which leads to a contribution of up to 60% to the total module cost, the solar cell manufacturers are forced to make a compromise between cost and performance. Consequently, obtaining efficiencies around 12% with a pure metallurgical silicon could be acceptable.

Acknowledgments

The authors thank Thomas Buck for having performed POCl_3 diffusion. The financial support of EU project FOXY (contract number 019811) is gratefully acknowledged.

References

- [1] B. Ceccaroli, O. Lohne, in: A. Luque, S. Hegedus (Eds.), *Handbook of Photovoltaic Science and Engineering*, John Wiley & Sons, England, 2003, pp. 153–204.
- [2] E.A. Meese, E.J. Øvrelid, H. Laux, M. M'Hamdi, *Proceedings of the 20th European Photovoltaic Solar Energy Conference*, 2005, pp. 909–913.
- [3] R.A. Sinton, A. Cuevas, M. Stuckings, *Proceedings of the 25th IEEE Photovoltaic Specialists Conference*, 1996, pp. 457–460.
- [4] T.S. Horányi, T. Pavelka und, P. Tüttö, *Appl. Surf. Sci.* 63 (1993) 306–311.
- [5] ASTM F43-93, 1996.
- [6] M. Acciarri, S. Binetti, A. Le Donne, S. Marchionna, M. Vimercati, J. Libal, R. Kopecek, K. Wambach, *Prog. Photovolt. Res. Appl.* 15 (2007) 375–386.
- [7] ASTM, F1391.93; ASTM F1188 93a.
- [8] LECO Corporation, *Application Bulletin* (1991).
- [9] I. Perichaud, *Sol. Energy Mater. Sol. Cells* 72 (2002) 315–326.
- [10] M. Sheoran, A. Upadhyaya, A. Rohatgi, *Solid State Electron.* 52 (2008) 612–617.
- [11] H. Nordmark, M. Di Sabatino, E.J. Øvrelid, J.C. Walmsley, R. Holmestad, *Proceedings of the 22th European Photovoltaic Solar Energy Conference*, vol. I, 2007, pp. 1710–1714.
- [12] M. Di Sabatino, A.L. Dons, J. Hinrichs, O. Lohne, L. Arnberg, *Proceedings of the 22nd European Photovoltaic Solar Energy Conference*, 2007, pp. 271–275.
- [13] M. Di Sabatino, S. Binetti, E.J. Øvrelid, M. Acciarri, J. Libal, *Proceedings of the 22nd European Photovoltaic Solar Energy Conference*, 2007, pp. 883–888.
- [14] C. Hassler, H.U. Hofs, W. Koch, G. Stollwerck, A. Muller, D. Karg, G. Pensl, *Mater. Sci. Eng. B* 71 (2000) 39–46.
- [15] G. Davies, *Phys. Rep.* 176 (1989) 83–188.
- [16] W. Kürner, R. Sauer, A. Dornen, K. Thonke, *Phys. Rev. B* 39 (1989) 13327–13337.
- [17] S. Pizzini, S. Binetti, E. Leoni, A. Le Donne, M. Acciarri, A. Castaldini, *MRS Symp. Proc.* 692 (2002) 275–281.
- [18] J. Weber, H.J. Queisser, *MRS Symp. Proc.* 59 (1986) 147–152.
- [19] M. Kittler, W. Seifert, *Mater. Sci. Eng. B42* (1996) 8–13.
- [20] J. Chen, T. Sekiguchi, D. Yang, F. Yin, K. Kido, S. Tsurekawa, *J. Appl. Phys.* 96 (2004) 5490–5495.
- [21] H. Nordmark, M. Di Sabatino, M. Acciarri, J. Libal, S. Binetti, E.J. Øvrelid, J.C. Walmsley, R. Holmestad, *Proceedings of the 33rd IEEE Photovoltaic Specialists Conference*, 2008, in press.
- [22] M. Sheoran, A. Upadhyaya, A. Rohatgi, *Solid State Electron.* 52 (2008) 612–617.
- [23] A. Borghesi, B. Pivac, A. Sassella, A. Stella, *J. Appl. Phys.* 77 (1995) 4169–4244.
- [24] P. Basore, P.D.A. Clugston, *PC1D v.5.9*, University of New South Wales (2003).